

Verification Of Forming Force, Major And Minor Strain For UHMWPE For Single Point Incremental Forming by Using Experimental And Analytical Approach.

Manoj P Bauskar¹, Prashant Singh², Shahid Ali³, Manish S Deshmukh⁴

^{1,2}Bir Tikendrajit University, Canchipur, Imphal West, 795003 (Manipur), India

^{3,4}All India Shri Shivaji Memorial Society's College of Engineering, Pune-411001 (MS), India.

¹mpbauskar@aissmscoe.com, ²Prashant.singhkalhans@gmail.com, ³saansari@aissmscoe.com,

⁴msdeshmukh@aissmscoe.com

Abstract: Mass Production is indeed need of every Industry such as automotive, Medical (artificial limb), aerospace, and appliances industries, which is in the form of conventional metal forming processes, such as Press work. However, for batch productions, novel flexible manufacturing processes, such as incremental sheet forming (ISF) must be utilized to decrease the production costs. Studying the process parameters in ISF process such as, the step size, tool size, feed rate, spindle speed, and wall angle is essential as they are affecting the formability and deformation behaviour of this process on UHMWPE which has promising application in medical field. The purpose of this study was to investigate the Spring Back, Twist, Dimensional Accuracy, forming limit diagram, comparison of experimental forming time and Analytical forming Time, comparison of Major Strain and Minor Strain commutated by experimental and analytical by using FEM and comparison of forming force computed by experimental and analytical by using FEM.

Keywords: SPIF; UHMWPE; Formability Limit Diagram; FEA.

INTRODUCTION:

The Single Point Incremental Forming (SPIF) method eliminates the need for dedicated punches or dies [1] and applies a controlled amount of plastic deformation to the sheet material, gradually shaping it into the desired final form. Due to the inherent flexibility of the Incremental Sheet Forming (ISF) process, it is possible to manufacture complex 3D geometries with a high degree of customization [2,3]. In Single Point Incremental forming sheet is formed with Hemispherical tool (single indenter) along with fixture [4]. One of the novel manufacturing methods is the Incremental Sheet Forming (ISF) process, where sheet metal is progressively formed using a VMC-operated forming tool [5,6]. This technique does not require dedicated dies, making it highly flexible and cost-effective for low-volume production, prototyping, and customized manufacturing. Besides experimental research, the behaviour and simulation of various sheet forming processes, such as stamping and incremental forming, are crucial for gaining a deeper understanding of deformation behaviour and optimizing forming conditions [8,9]. The purpose of this study is to investigate Forming Limit Diagram of UHMWPE, computation of tool force, forming time and major and minor strain experimentally and analytically (FEM). In recent decades, the application of Single Point Incremental Forming (SPIF) to polymeric materials has grown considerably. This increase is due not only to the advantages of the process but also to experimental evidence showing that the strains achieved through SPIF surpass the Forming Limit Curve (FLC) without leading to material failure [10–11]. As noted by Marques et al. [10], polymeric sheets often exhibit delayed or even completely suppressed necking. Consequently, the conventional FLC does not effectively represent formability in this case. Instead, the Fracture Forming Line (FFL) is typically used to define the formability limits of polymeric sheets within the principal strain space, accounting for their distinct deformation characteristics. In the context of the SPIF process for polymers with conical geometries, Martins et al. [12] identified three principal failure modes. The first, circumferential cracking, occurs when cracks form along the circumferential direction. The second, twisting or wrinkling, takes place when the material twists inside the cone, leading to wrinkle formation on the part's walls. The third, oblique cracking, is characterized by cracks forming along the bisector direction on the inclined wall. Among these, circumferential cracking and twisting are the most frequently observed failure modes in SPIF. Le et al. [13] reported both failure modes in cone-shaped parts with a circular arc generatrix, using a 3 mm thick polypropylene (PP) sheet. Similarly, Davarpanah et al. [14] examined two SPIF geometries—a variable wall angle and a fixed-angle

conical geometry—using 0.7 mm thick polylactic acid (PLA) sheets, and identified the same failure patterns. Beyond these common failure modes, Rosa-Sainz et al. [15] discovered an additional failure mechanism, known as crazing, in PC sheets subjected to SPIF. Their study investigated PC sheets with a thickness of 2 mm and a truncated conical geometry while varying spindle speeds at 20, 500, and 1000 rpm. The results indicated that crazing occurred exclusively at 1000 rpm, causing multiple micro-cracks to develop on the deformed specimen. These findings highlight the challenges and potential failure mechanisms involved in SPIF when applied to polymer sheets. With the increasing focus on SPIF process analysis, numerous studies have explored its applications in the medical field, particularly for manufacturing customized prostheses using incremental forming techniques with polymeric biomaterials. These materials must be biocompatible, meaning they should be able to interact with human tissues over extended periods without adverse effects [16]. Several researchers, including Bagudanch et al. [17], Centeno et al. [18], Clavijo-Chaparro et al. [19], and Chen et al. [20], have investigated the use of SPIF for fabricating polymeric sheets for cranial prostheses. Additionally, Fiorentino et al. [21] conducted a study on biocompatible biomedical devices produced via Incremental Sheet Forming (ISF), specifically examining the manufacture of a palate prosthesis using a combination of titanium alloy and polycaprolactone (PCL), with promising results. In medical applications, Ultra-High Molecular Weight Polyethylene (UHMWPE) is widely used in orthopedic implants such as hip, knee, shoulder, elbow, wrist, ankle, and spinal disk replacements due to its superior properties [22]. UHMWPE is highly valued for its exceptional wear resistance, low friction coefficient, biocompatibility, and high impact strength [23], making it a preferred material for joint replacement components and orthopedic devices. The introduction of UHMWPE as a bearing material for total joint replacements by Charnley [24] in 1962 marked a significant advancement, and it has since become the gold standard for articulating surfaces in total hip, knee, and shoulder prostheses.

METHODOLOGY

2.1 Experimental Method: The Incremental Sheet Forming (ISF) tests were conducted using a FEELER VMP-40A Vertical Machining Center, located at Sabicorp, Pune (412216) as shown in Figure 1. The experimental setup incorporated a robust clamping system (illustrated in Figure 2a) to securely hold the UHMWPE sheet during the forming process. A specialized fixture was employed for this purpose, ensuring stability and minimizing any undesired movements of the polymer sheet. During the tests, the servo load factors along the spindle axes (x, y, and z) were carefully recorded. These load factors provided critical data for estimating the cutting forces exerted along each axis (F_x , F_y , and F_z). Among these, the force along the z-axis (F_z) was particularly significant as it directly influenced the forming process. For each experimental run, the F_z values were meticulously measured to analyze their impact on the material deformation and the overall forming performance. Tests were conducted on 1 mm-thick sheets of Ultra-High Molecular Weight Polyethylene (UHMWPE), a widely recognized biocompatible polymer. The experimental setup employed a conical frustum as the test geometry, as illustrated in Figure 1a. This geometry was characterized by an initial wall angle of 45° , which progressively increased to 50° . The blank material used for the tests had dimensions of 100 mm x 100 mm, ensuring uniformity in sample size. A spiral tool path was implemented during the experiment to achieve consistent material deformation and precise geometry formation. The conical frustum geometry, combined with the spiral tool path, was chosen to evaluate the material's forming capabilities and response under specific loading conditions. These features highlight the meticulous design of the experimental procedure to study the mechanical behaviour and adaptability of UHMWPE in advanced applications.



Figure 1.FEELER VMP-40A Vertical Machining Centre.

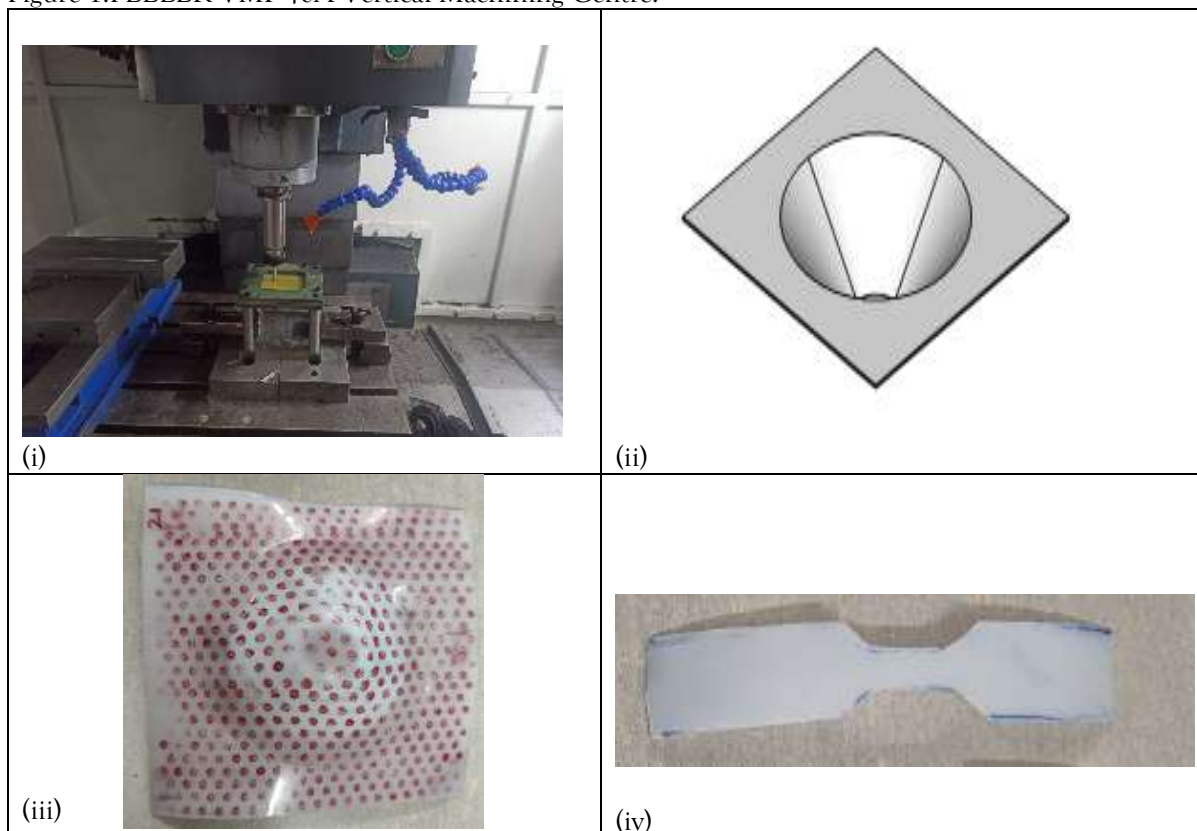


Figure 2. (a) Fixture (b) Test Geometry (c) UHMWPE part (d) Tensile Test Specimen.

2.1.1 Material Properties: The tensile test is carried out according to ASTM rectangular dog-bone shaped samples of the UHMWPE were performed to obtain the stress-strain curves [25]. Tests were done on Universal Testing Machine for plotting stress strain curve shown in

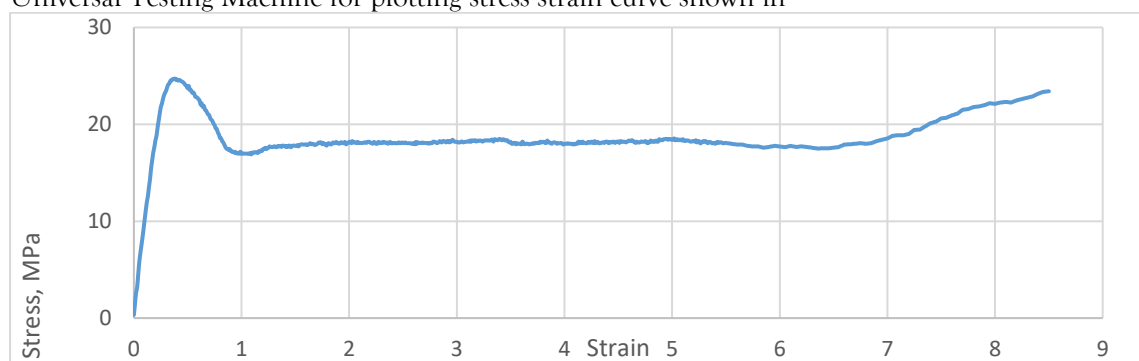


Figure 3. Stress Strain Curve

From the point of view of mechanical behaviour, UHMWPE shows strain hardening behaviour after yield point and is valued as more rigid material.

Table 1. Mechanical properties.

Material	Tensile Strength (MPa)	Elastic Modulus (MPa)
UHMWPE	25.59	119

2.2. Design of Experiments

In this study, the Taguchi L27 orthogonal array was utilized to systematically investigate the Single Point Incremental Forming (SPIF) process for UHMWPE sheets. The experimental design was carefully developed to explore the influence of various process parameters on forming performance. The explanatory variables for the study were selected based on classical approaches commonly employed in Incremental Sheet Forming (ISF) research for metals. This ensured that the methodology aligned with established practices while accommodating the unique characteristics of UHMWPE as a polymer material. To maintain consistency and facilitate direct comparison across experiments, the sheet thickness was held constant at 1 mm. This approach eliminated variability associated with material thickness, focusing the investigation on other influential parameters. Spindle speed was included as a key variable in the study, as it plays a critical role in the forming of polymer sheets. The spindle speed directly affects the material's deformation behaviour, heat generation, and surface finish, making it a crucial factor in optimizing the SPIF process. The levels of the selected variables were carefully defined to ensure comprehensive coverage of the parameter space while maintaining practical feasibility. This systematic approach allowed for a detailed analysis of how each variable and their interactions influenced the forming performance, material response, and overall process efficiency. By employing the Taguchi L27 orthogonal array, the study effectively reduced the number of experimental runs required while ensuring statistically robust results, paving the way for insights into the optimal parameters for forming UHMWPE sheets using SPIF. Table 2: Process Parameters. DOE table is shown in Table 3a.

Table 2 Process Parameters.

Parameters	Levels		
F: Feed (mm/min)	400	600	800
S: Spindle Speed(rpm)	400	600	800
D: Tool Diameter (mm)	8	10	12
Z: Step size(mm)	0.5	0.75	1

Table 3a. Design of Experiment.

Run	Tool Diameter (D)	Spindle Speed (S)	Feed Rate (F)	Step Size (Z)
1	8	400	400	0.5
2	8	400	600	0.75
3	8	400	800	1
4	8	600	400	0.75
5	8	600	600	1
6	8	600	800	0.5
7	8	800	400	1
8	8	800	600	0.5
9	8	800	800	0.75
10	10	400	400	0.5
11	10	400	600	0.75
12	10	400	800	1
13	10	600	400	0.75
14	10	600	600	1
15	10	600	800	0.5
16	10	800	400	1

17	10	800	600	0.5
18	10	800	800	0.75
19	12	400	400	0.5
20	12	400	600	0.75
21	12	400	800	1
22	12	600	400	0.75
23	12	600	600	1
24	12	600	800	0.5
25	12	800	400	1
26	12	800	600	0.5
27	12	800	800	0.75

Computation of Major & Minor Strain In Table 3b Experimental computed value of Major strain & Minor strain is shown below High major strain is observed for Tool Diameter 12 mm and at 800 mm/min of Feed Rate for Experimental run 21 values are arranged as per descending order.

Table 3b. Experimental value of Major and Minor Strain

Experiment Run	Tool Diameter mm	Spindle Speed rpm	Feed Rate mm/min	Step Size Down mm	Minor Strain	Major Strain
21	12	400	800	1	-0.510825624	0.936093359
23	12	600	600	1	-0.430782916	0.875468737
22	12	600	400	0.75	-0.287682072	0.667829373
10	10	400	400	0.5	-0.223143551	0.530628251
6	8	600	800	0.5	-0.162518929	0.470003629
1	8	400	400	0.5	-0.105360516	0.438254931

Formability Limit Diagram is plotted as per experimental data obtained can be seen below shown Figure 4

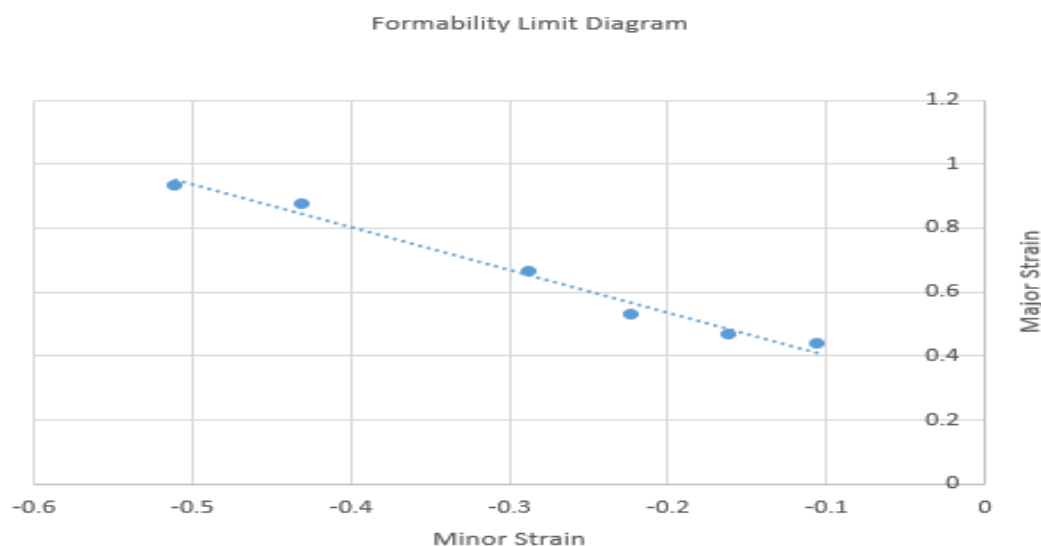


Figure 4. Formability Limit Diagram for UHMWPE

2.3 Finite Element Simulation of SPIF Process: An explicit dynamic approach was used to simulate the SPIF process to produce a conical geometry with 50 ° angle, 30 mm depth, and 70 mm upper diameter with a tool, modelled as a rigid body, with hemispherical head of 12 mm in diameter and feed rate of 400 mm/s. The sheet metal was assumed to be UHMWPE Both the sheet and the tool were simulated using

shell elements, the main characteristics of the FEM model (properties of the elements and of the materials, boundary, and contact conditions) are reported in Table 4a.

Table 4a. Main Properties of the FEM parts

Part	Sheet	Tool
Element Type	S4R	3D Analytical Rigid Shell
Integration points on the surface	4	
Integration points through thickness	1	
Number of elements	2500	
Mean dimension of elements	1	
Material model	Mat Plasticity Polymer	
Density[g/cm ³]	0.940	
Young Modulus [MPa]	114	
Poisson's Ratio	0.25	
Yield Stress[MPa]	16.9	
Ultimate elongation	603	
Boundary condition	Rotational & translation constraint encastered along X,Y & Z translations for rigid part	
Contact conditions	Surface to Surface friction coefficient =0.05	


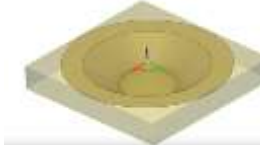

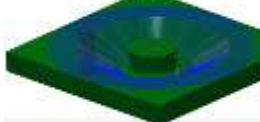
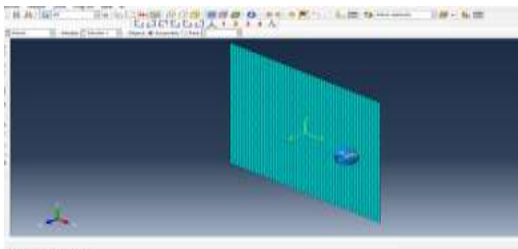
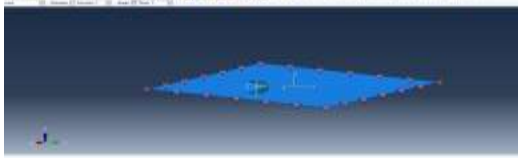
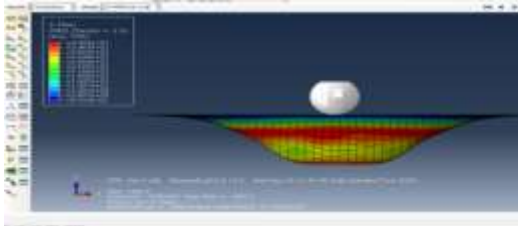
Following step by step approach is used for simulation. First model is created in creo as per drawing then imported in Fusion 360 for generation of tool path first define stock 100 mm x100 mm in new set up for creating cone geometry. Then select spiral tool path and here defining tool as ball nose tool by defining diameter of tool, Speed 600 rpm , feed 400 min/s. After this select forming area for actual forming and also define type of milling and step size 0.75 and movement of tool from outside to in. Do Post processing for creation of file to get position coordinates and file in the form of note pad is converted by G code ripper software in required csv type file for getting x,y and z co-ordinates. Then to create position file for Abacus calculate total distance between x,y and z point also calculate time between two points by using following formula $Velocity = \frac{Distance}{Time}$ by doing this will get total time for complete simulation. Now in Abaqus version 6.14.5 is used and following step by step approach is used as shown in Table 4 for analytical simulation.

Table 4 b. Approach for simulation in Abaqus

Step	Process
1	Model creation of sheet 100*100 mm, 1 mm thick.
2	Tool modelling as rigid surface
3	Assembly and contact definition (friction=0.25, normal behaviour)
4	Material Property assignment defining Mesh size 1mmx1mm
5	Step definition: Time of analysis (from fusion)
6	Definition of displacement boundary condition for tool (displacement from fusion) and sheet (encastre).

In Table No 5 Procedure for simulation is explained as per following details with figure.

Table 5. Procedure for Simulation

Sr No	Process	Particulars/ Geometry
1	Geometry In Fusion 360	
2	Defining Stock In Fusion 360	
3	Defining tool	
4	Creation of tool path	
5	Model creation of sheet 100*100 mm, 1 mm thick, Tool modelling as rigid surface, Material Property assignment, Mesh	
6	Load and displacement boundary condition	
7	Run for Result	

RESULT & DISCUSSION

3.1 Comparison of Experimental & Analytical Forming Time: Forming time is time required to form the blank into finish job. In Table 6 and Figure 5 it is clear that there is very less deviation between forming time which is computed Experimental & Analytical, they agree well with each other.

Table 6. Comparison of Experimental & Analytical Forming Time

Run	Tool Diameter (D)	Spindle Speed (S)	Feed Rate (F)	Step Size (Z)	Experimental Forming Time	Analytical Forming Time
1	8	400	400	0.5	1188	1192
2	8	400	600	0.75	540	544
3	8	400	800	1	313	316
4	8	600	400	0.75	801	806
5	8	600	600	1	411	417
6	8	600	800	0.5	604	608
7	8	800	400	1	607	612
8	8	800	600	0.5	799	804
9	8	800	800	0.75	410	415
10	10	400	400	0.5	1162	1166
11	10	400	600	0.75	528	533
12	10	400	800	1	306	310
13	10	600	400	0.75	783	788
14	10	600	600	1	402	406
15	10	600	800	0.5	590	595
16	10	800	400	1	594	598
17	10	800	600	0.5	781	785
18	10	800	800	0.75	401	406
19	12	400	400	0.5	1136	1141
20	12	400	600	0.75	517	521
21	12	400	800	1	300	306
22	12	600	400	0.75	765	770
23	12	600	600	1	393	397
24	12	600	800	0.5	577	580
25	12	800	400	1	580	582
26	12	800	600	0.5	763	766
27	12	800	800	0.75	392	395

In the below mentioned figure 5 Graph is plotted Experimental run verses Experimental & Analytical forming time on X axis and Y axis respectively.

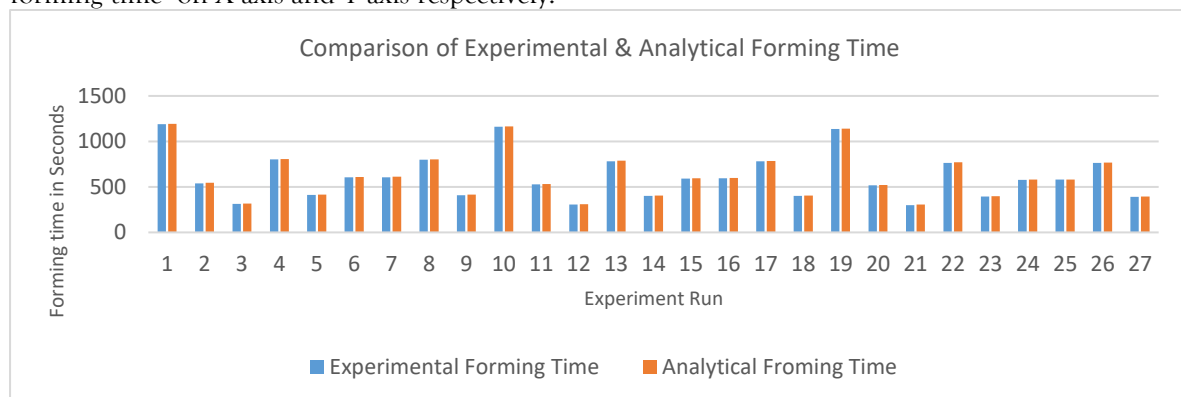


Figure5. Comparison of Experimental & Analytical Forming Time.

3.2 Comparison of Experimental & Analytical computed Major Strain and Minor Strain: Major and Minor Strain is computed for Run no 22 experimentally & analytical shown in below mentioned table no 7. In the below figure 6a and 6b Major strain & Minor strain are calculated by FEM is shown. They agree well with each other as shown in Table no7.

Table .7 Comparison of Experimental & Analytical for Major & Minor Strain

Experiment Run	Analytical Result		Experimental result		% Deviation	
	Minor Strain	Major Strain	Minor Strain	Major Strain	Minor Strain	Major Strain
22	-0.313	0.647	-0.28768	0.6678	8%	3.3%

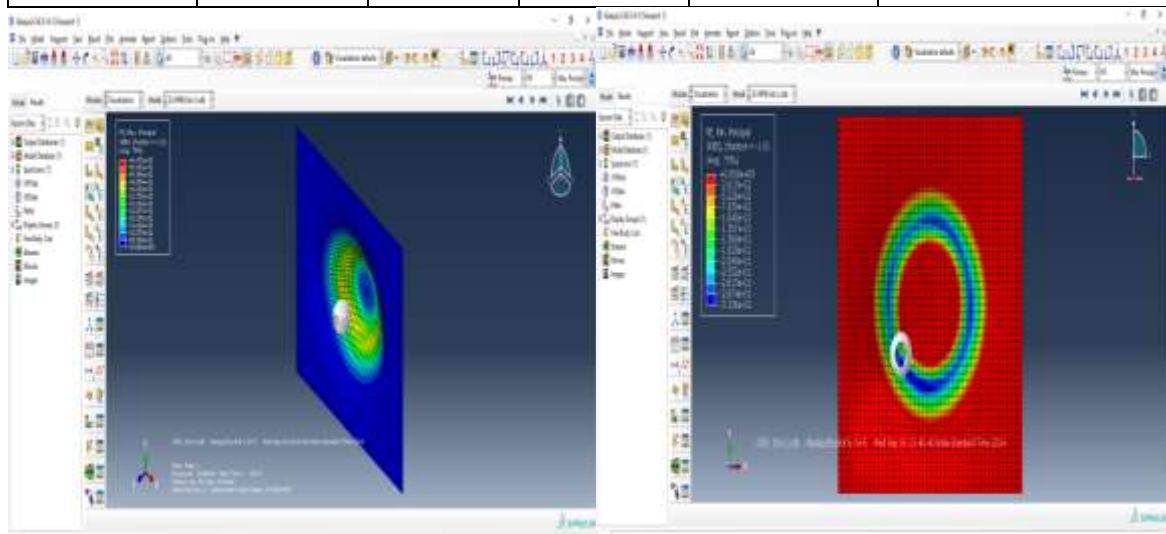


Figure 6a Major Strain by Analytical method Figure 6b Minor Strain by Analytical method

3.3 Comparison of Experimental & Analytical Computed Tool Force: Tool Force is computed for Run no 22 experimentally & analytical shown in below mentioned table no 8. Which shows that Tool force computed analytically & experimentally agrees closely with each other.

Table 8 Comparison of Experimental & Analytical for Tool Force.

Experiment Run	Analytical Result	Experimental result	% Deviation
	Tool Force	Tool Force	Tool Force
22	244	243	0.41

Figure 7 shows tool force for Experiment run no 22 which is computed by analytically.

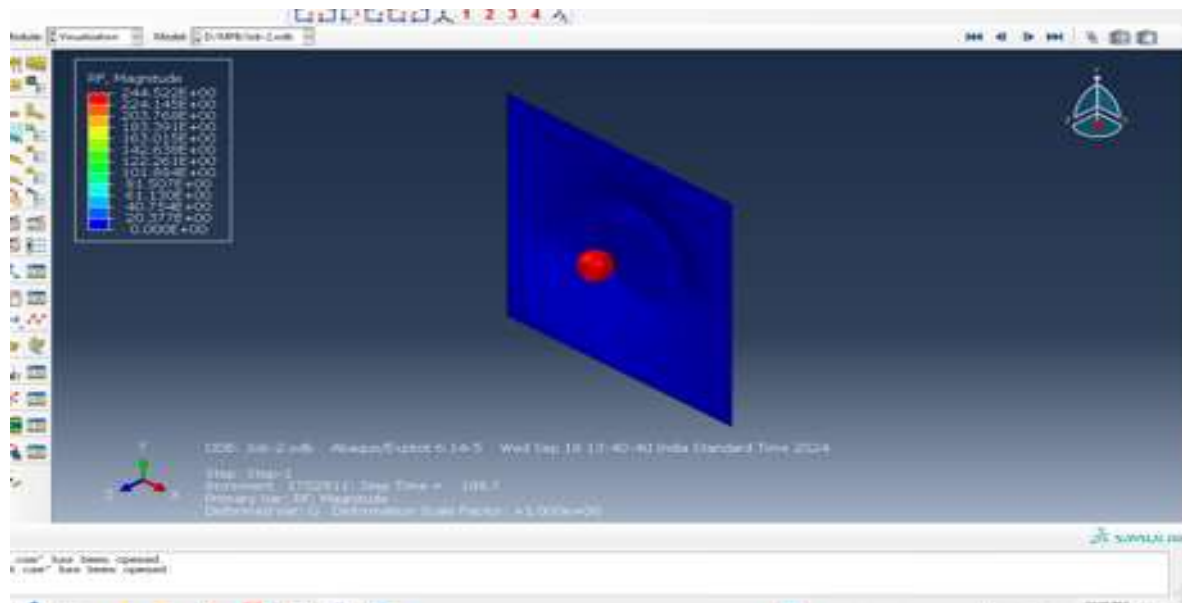


Figure 7 Tool force computed by FEM

CONCLUSION

Forming Time: In this research the Experimental and analytical computed forming time agrees with each other very well, and it is clearly noted that there is very close relation between them. The maximum percentage deviation is for run 5 is noted 1.45%.

Forming Limit Diagram: Forming Limit Diagram is successfully constructed for Single Incremental forming by plotting grid of Circle on given blank and after incremental forming process major and minor strain are computed.

It is noted that Major and Minor strain computed by experimentally for run 22 and analytically (FEM) has Percentage deviation of 3.3% and 8% respectively.

Forming Force: It is clear that the Tool force computed by experimental and Analytical (FEM) agrees well with each other. The Percentage deviation for Run 22 is 0.41%.

REFERENCES

- [1] Park J J, Kim Y H 2003 Fundamental studies on the incremental sheet metal forming technique J. Mater. Process. Technol. 140 447-453
- [2] Umakant Dinkar Butkar, et.al "Accident Detection and Alert System (Current Location) Using Global Positioning System" JOURNAL OF ALGEBRAIC STATISTICS Vol. 13 No. 3 (2022) e-ISSN: 1309-3452.
- [3] A. K. Bhaga, G. Sudhamsu, S. Sharma, I. S. Abdulrahman, R. Nittala and U. D. Butkar, "Internet Traffic Dynamics in Wireless Sensor Networks," 2023 3rd International Conference on Advance Computing and Innovative Technologies in Engineering (ICACITE), Greater Noida, India, 2023, pp. 1081-1087, doi: 10.1109/ICACITE57410.2023.10182866.
- [4] Hagan E, Jeswiet J 2003 A review of conventional and modern single-point sheet metal forming methods Proc. Inst. Mech. Eng. Part B J. Eng. Manuf. 217 213-225
- [5] Butkar, M. U. D., & Waghmare, M. J. (2023). Advanced robotic manipulator renewable energy and smart applications. Computer Integrated Manufacturing Systems, 29(2), 19-31.
- [6] D. S. Thosar, R. D. Thosar, P. B. Dhamdhare, S. B. Ananda, U. D. Butkar and D. S. Dabhade, "Optical Flow Self-Teaching in Multi-Frame with Full-Image Warping via Unsupervised Recurrent All-Pairs Field Transform," 2024 2nd DMIHER International Conference on Artificial Intelligence in Healthcare, Education and Industry (IDICAIEI), Wardha, India, 2024, pp. 1-4, doi: 10.1109/IDICAIEI61867.2024.10842718.
- [7] P. B. Dhamdhare, D. S. Thosar, S. B. Ananda, R. D. Thosar, D. S. Dabhade and U. D. Butkar, "A Semantic Retrieval System Using Imager Histogram Computation to reduce Trademark infringement based on the conceptual similarity of text," 2024 2nd DMIHER International Conference on Artificial Intelligence in Healthcare, Education and Industry (IDICAIEI), Wardha, India, 2024, pp. 1-6, doi: 10.1109/IDICAIEI61867.2024.10842701.
- [8] Kim H, Park T, Esmailpour R and Pourboghra F 2018 Numerical Study of Incremental Sheet Forming Processes J. Physics: Conf. Series. 1063 012017
- [9] Mohammed B, Park T, Pourboghra F, Hu J, Esmailpour R and Abu-farha F 2017 Multiscale crystal plasticity modeling of multiphase advanced high strength steel strength steel Int. J. Solids and Structures.000 1-19

- [10] Marques, T.A.; Silva, M.B.; Martins, P.A.F. On the Potential of Single Point Incremental Forming of Sheet Polymer Parts. *Int. J. Adv. Manuf. Technol.* 2012, 60, 75–86.
- [11] Centeno, G.; Morales-Palma, D.; Gonzalez-Perez-Somarriba, B.; Bagudanch, I.; Egea-Guerrero, J.J.; Gonzalez-Perez, L.M.; García Romeu, M.L.; Vallengano, C. A Functional Methodology on the Manufacturing of Customized Polymeric Cranial Prostheses from CATUsing SPIF. *Rapid Prototyp. J.* 2017, 23, 771–780
- [12] Martins, P.A.F.; Kwiatkowski, L.; Franzen, V.; Tekkaya, A.E.; Kleiner, M. Single Point Incremental Forming of Polymers. *CIRP Ann. Manuf. Technol.* 2009, 58, 229–232.
- [13] Le, V.S.; Ghiotti, A.; Lucchetta, G. Preliminary Studies on Single Point Incremental Forming for Thermoplastic Materials. *Int. J. Mater. Form.* 2008, 1, 1179–1182.
- [14] Davarpanah, M.A.; Mirkouei, A.; Yu, X.; Malhotra, R.; Pilla, S. Effects of Incremental Depth and Tool Rotation on Failure Modes and Microstructural Properties in Single Point Incremental Forming of Polymers. *J. Mater. Process. Technol.* 2015, 222, 287–300.
- [15] Rosa-Sainz, A.; Centeno, G.; Silva, M.B.; Vallengano, C. Experimental Failure Analysis in Polycarbonate Sheet Deformed by Spif. *J. Manuf. Process.* 2021, 64, 1153–1168.
- [16] Tathe, A.; Ghodke, M.; Nikalje, A.P. A Brief Review: Biomaterials and Their Application
- [17] Bagudanch, I.; Garcia-Romeu, M.L.; Ferrer, I.; Ciurana, J. Customized Cranial Implant Manufactured by Incremental Sheet Forming Using a Biocompatible Polymer. *Rapid Prototyp. J.* 2018, 24, 120–129
- [18] Centeno, G.; Bagudanch, I.; Morales-Palma, D.; García-Romeu, M.L.; Gonzalez-Perez-Somarriba, B.; Martinez-Donaire, A.J.; Gonzalez-Perez, L.M.; Vallengano, C. Recent Approaches for the Manufacturing of Polymeric Cranial Prostheses by Incremental Sheet Forming. *Proc. Procedia Eng.* 2017, 183, 180–187
- [19] Clavijo-Chaparro, S.L.; Iturbe-Ek, J.; Lozano-Sánchez, L.M.; Sustaita, A.O.; Elías-Zúñiga, A. Plasticized and Reinforced Poly(Methyl Methacrylate) Obtained by a Dissolution-Dispersion Process for Single Point Incremental Forming: Enhanced Formability towards the Fabrication of Cranial Implants. *Polym. Test.* 2018, 68, 39–45.
- [20] Chen, L.F.; Chen, F.; Gatea, S.; Ou, H. PEEK Based Cranial Reconstruction Using Thermal Assisted Incremental Sheet Forming. *Proc. Inst. Mech. Eng. Part B J. Eng. Manuf.* 2021, 236, 997–1004.
- [21] Fiorentino, A.; Marenda, G.P.; Marzi, R.; Ceretti, E.; Kemmoku, D.T.; Lopes Da Silva, J.V. Rapid Prototyping Techniques for Individualized Medical Prosthesis Manufacturing. In *Innovative Developments in Virtual and Physical Prototyping, Proceedings of the 5th International Conference on Advanced Research in Virtual and Rapid Prototyping, Leiria, Portugal, 28 September–1 October 2011*; CRC Press: Boca Raton, FL, USA, 2012; Volume 1, pp. 589–594.
- [22] Chilukoti, G.R.; Periyasam, A.P. Ultra High Molecular Weight Polyethylene for Medical Applications.
- [23] Kurtz, S.M. From Ethylene Gas to UHMWPE Component: The Process of Producing Orthopedic Implants. In *UHMWPE Biomaterials Handbook: Ultra High Molecular Weight Polyethylene in Total Joint Replacement and Medical Devices: Third Edition*; William Andrew Publishing: Norwich, NY, USA, 2016; pp. 7–20. ISBN 9780323354011.
- [24] Musib, M.K. A Review of the History and Role of UHMWPE as A Component in Total Joint Replacements. *Int. J. Biol. Eng.* 2011, 1, 6–10.
- [25] Esmaeilpour R, Kim H, Park T, Pourboghraat F, Xu Z, Mohammed B and Abu-Farha F 2018 Calibration of Barlat Yld2004-18P Yield Function Using CPFEM and 3D RVE for the Simulation of Single Point Incremental Forming (SPIF) of 7075-O Aluminum Sheet *Int. J. Mech. Sci.* 145 24–41